MR-Integrated Linear Accelerators: First Clinical Results

7

Olga Pen, Borna Maraghechi, Lauren Henke, and Olga Green

7.1 Introduction

Harold Johns from Ontario Cancer Institute once said, "If you can't see it, you can't hit it, and if you can't hit it, you can't cure it". No truer words have been spoken in the world of radiation therapy when it comes to cancer, and the paradigm of improving the imaging techniques as the means of narrowing down the target that needs to be irradiated in order to reliably cure cancer has been the moving force behind the invention of the adaptive treatment workflow. After all, by accounting for the changes in the patient's anatomy on the day-to-day basis, both the precise delivery of the maximum dose to the target with the simultaneous significant reduction of the dose to the surrounding tissue can be achieved, providing for both the reduced toxicity and a possibility of the dose escalation and shorter treatment times. The majority of the radiation treatment system employs computed tomography (CT)-based imaging in order to delineate the target and calculate the necessary radiation dose; however, it comes with certain limitations. Photon scattering has been long plaguing the quality of the CT images, providing for the poor contrast between the different soft tissues and necessitating the reliance on the implanted fiducial markers when considering the target for adaptive treatment prospects. Utilizing other imaging modalities might prove to the key to solving that particular problem, with magnetic resonance imaging (MRI) in particular coming to mind as a versatile tool in providing us with deeper information about the soft tissue contrast. Currently, there are several commercially available linear accelerator (LINAC) systems incorporating

O. Pen (✉)
Atrium Health, Huntersville, NC, USA

Washington University in St Louis, St Louis, MO, USA

B. Maraghechi · L. Henke · O. Green
Washington University in St Louis, St Louis, MO, USA
e-mail: borna.maraghechi@wustl.edu; henke.lauren@wustl.edu; ogreen@wustl.edu

E. G. C. Troost (ed.), *Image-Guided High-Precision Radiotherapy*,
https://doi.org/10.1007/978-3-031-08601-4_7

an MRI scanner (MR-LINAC), with the magnetic field strength ranging from 0.35 Tesla (T) to 1.5 T (see Chap. 6). Lower magnetic strength allows for the normal operation of linear accelerator, preventing the electron path distortion and allowing for a precise calculation of the radiation dose; however, it inevitably affects the image quality. A compromise must be reached so that the image quality is still sufficient for the purpose of target and organs-at-risk (OAR) delineation in real time, allowing for fraction-to-fraction adaptation with patient never leaving the treatment table while the new plan based on the day-to-day anatomical variation is devised. Several problems need to be solved in order to make it a possibility, with key elements of the adaptive treatment being subdivided into imaging, assessment, replanning, and quality assurance. Overall the workflow of the adaptive radiation treatment can be summarized by the following diagram [1] (Fig. 7.1).

When it comes to imaging, the problem can be further subdivided into the image quality assurance in general and ensuring the imaging suitability for the purposes of the adaptive treatment in particular. For instance, gating is a powerful tool that allows to incorporate the natural breathing pattern and associated anatomical variations and target movement. Incorporating the gating capabilities in the operation of MR-LINAC is an important step of making the adaptive treatment a reality. Significant effort is devoted to develop real-time three-dimensional MRI techniques that minimize the imaging latency and allow decreasing the computational time required to adapt the treatment pattern to the current anatomy. One of the unique challenges of the adaptive radiation treatment is the need to immobilize patient for the duration of the full workflow, which can be further exacerbated by the claustrophobia and discomfort associated with the extremely limited space inside the MR-LINAC bore. Thus, the imaging strategy has to be robust in order to account for patient's involuntary movement [2].

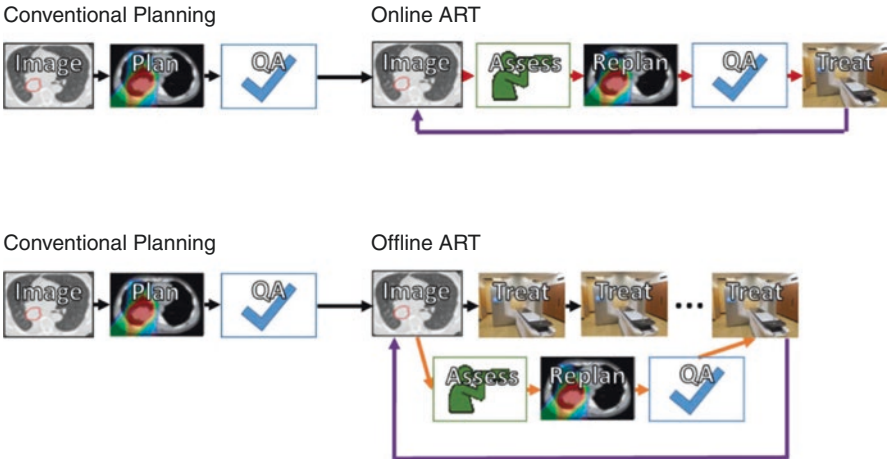

Fig. 7.1 Adaptive workflow—online and offline [1]. Image used with permission

The next question to be considered when devising the strategy for online adaptive treatment with the use on MR-LINAC is the exact imaging technique to use for the target and OAR assessment to determine if radiation treatment adaptation is even required. A wide variety of different sequences exist in the world of diagnostic MRI; however, due to the time constraints, not all of them are well adapted for the time-constrained environment of the online adaptive radiation therapy. The common techniques used these days include T1- and T2-weighted images, dynamic contrast-enhanced MRI for vasculature visualization, chemical effect saturation transfer (CEST) MRI for mobile protein and peptide content, as well as tumor hypoxia tracing, diffusion-weighted imaging, as well as many other less common modalities [3]. As of this moment, however, T1- and T2-weighted images remain to be most commonly used for the purposes of radiation treatment adaptation, though that might change as the technology of image acquisition and reconstruction continues to improve. The emergence of radiogenomics and imaging genomics is also a developing field that might be particularly helpful in the future with devising the adaptive radiation treatment for patients with glioblastoma, as well as other sites, as the field continues to develop. MRI fingerprinting for the multiple biomarker mapping might become a reality in the nearest future.

When it comes to replanning, several unique challenges arise. One such concern specific to radiation treatment in MR-LINACs in particular is the electron return effect that adds to the computational burden when assessing the dose at the interface of the tissues with highly varying electron densities. Monte Carlo simulation solution seems to be the most accurate from the calculation algorithms currently present on the market; however, the time constraints are imminent when considering the MR-LINAC application for the online adaptive radiation treatment, and not as much time can be devoted to recalculating the dose and optimizing the multileaf collimator (MLC) leaf pattern as would be common for the offline radiation treatment planning.

The real-time quality assurance has to rely on the extensive use of the Monte Carlo simulation as well as the customary dose measurement common to the intensity-modulated radiation therapy (IMRT)-based treatment is unavailable with the adaptive treatment workflow. Portal dosimetry and exit dose analysis, as well as extensive machine logs, become an absolute necessity.

7.2 Clinical Sites

All of these challenges contribute to the necessity to improve and develop better adaptive treatment protocols and strategies. Nevertheless, the movement to use MR-LINACs for adaptive treatment is gaining momentum in the field of radiation oncology, with new reports of a successful implementation appearing in the literature. Numerous clinical trials are being conducted on various anatomical sites to assess the suitability of using the MRI-guided adaptive radiation treatment at this moment, and summary of some of these trials and clinical cases is presented in this chapter in the form of review on site-by-site basis [1, 4].

7.2.1 Brain and Spine

Radiation treatment is a common strategy for dealing with the tumors of the central nervous system in general and brain tumors in particular. Both primary and metastatic tumors of the brain have long been benefiting from MRI imaging for target delineation and OAR sparing. MRI scan obtained via a diagnostic scanner is typically registered to the CT scan via bony anatomy with high degree of confidence and can then be used for contouring. As the target is unlikely to move within the rigid structure of the brain, the most common consideration for the need for the adaptive treatment comes from the target size change postresection, if a significant time has passed between the diagnostic scan and the day of treatment, or the target size assessment of the fraction to fraction basis in case of multifraction stereotactic body radiotherapy (SBRT; typically 3–5 fractions; fx). Mehta et al. [5] present a study on several cases of grade 4 glioblastoma patients postresection, with the changes of the resection cavity size, tumor volume and cerebral edema being tracked via MR-LINAC imaging capabilities. The daily decrease in the cavity measurement was observed in all patients and was significant enough to justify the additional costs of the adaptive treatment for the improved tumor control and toxicity decrease. These results are consistent with results previously obtained with the help of diagnostic MRI scans mid-treatment by Tsien et al. [6], Shukla et al. [7], and Yang et al. [8]. Another study was performed by Maziero et al. [9] on conventionally fractionated RT conducted on MR-LINAC with the MRgRT (MR-guided radiotherapy) scans obtained to identify serious pathologies and edema changes during the course of treatment, highlighting the evolution in the tumor volume following the course of radiation treatment and providing recommendations for gross tumor volume (GTV) adaptation. The authors discuss the possibility of physiologic adaptive radiotherapy as the future venue for the treatment of brain tumors. In addition, a presentation of the cases of the spine adaptive treatment, with a focus on bowel OAR migration, has been presented. Another study by Spieler et al. [10] also presents the cases of the SBRT treatment of the spinal metastases conducted on 0.35 T MRI-RT Co-60 system. In addition to the advantages of more precise target delineation and OAR sparing, authors noted that MR-LINAC-generated images had the additional advantages of using the low-field MRI to mitigate the magnetic susceptibility artifacts caused by the spinal hardware.

7.2.2 Head and Neck

The first studies related to the use of MR-LINAC on head and neck patients date back to 2016, when six patients were observed during the course of IMRT treatment by Raghavan et al. [11]. At that time, the pretreatment MRIs on selected fractions were performed and the changes in the GTV and parotid glands were delineated. A significant shrinkage of GTV and parotid gland volume was observed, establishing the need for the treatment planning adaptation in the future. In 2017, a more thorough clinical trial involving the use of the Co-60 Viewray MR-LINAC on head and

neck patients was performed by Chen et al. [12]. At that time, 18 patients received the standard IMRT radiation courses with the target and OAR delineation being manually adjusted by the attending physician on the day-to-day basis. Two of the patients also had functional MRI data obtained via diffusion-weighted sequences on a weekly basis. All of the patients were followed up for 18-month postcompletion, with positron emission tomography (PET) scans obtained approximately 3-months postcompletion, and quality of life assessments performed periodically. All of the patients demonstrated the treatment results comparable to one with the conventional IMRT treatment, with quality of life being rated either very good or outstanding for 70% of the patients, thus validating the feasibility of the MR-guided radiation therapy [12]. This study was followed by several other studies exploring different aspects of the adaptive treatment planning and delivery process when performed on the head and neck cases. A study performed by Chamberlain et al. [13] established that increasing the number of segments and beams increased the dose conformality without prolonging the overall treatment time. A study by Gurney-Champion et al. [14] helped to determine the extent of the 3D intrafractional motion of the head and neck patients to determine the effect of the increased treatment time for the adaptive treatment on the patient's ability to retain the position for the minimal movement of the tumor. The results of the assessment showed that both the systematic and random motions were well within the clinical safety margins. Another study to determine the radiation treatment margins for head and neck tumors was performed by Bruijen et al. [15]. A first adaptive radiation treatment study using 1.5 T Elekta Unity MR-LINAC was performed by McDonald et al. [16] and confirmed the feasibility of the previously established margins. At that time, 10 patients received treatment. Seven patients received at least one treatment with the backup plan on a conventional LINAC owing to the machine downtime or admittance to inpatient facilities. All patients were treated with online adaptive treatment workflow. Doses to all OARs were consistent between the reference plan and summation plan. Significant tumor shrinkage, weight loss, and anatomical deformations were observed but were able to be accounted for with the use of adaptive treatment workflow. Parotid glands and spinal cord were specifically benefited from the treatment adaptation. Treatment times were less than an hour in 91% of the cases. These results were consisted with the similar online adaptation workflow results performed on the ViewRay 0.35 T MR-LINAC. Several other studies are currently being performed in order to establish the protocols for safe dose reduction without the sacrifice in tumor control.

7.2.3 Thoracic Tumors

The thoracic region presents unique challenges when it comes to MRI. The respiratory motion introduces an uncertainty that often requires increased planning target volume (PTV) margins, and the variability of the anatomy in the region on the day-to-day basis introduces the possibility of the high degree of toxicity. Technical challenges and solutions associated with MR-guided radiation treatment in the thorax

include, e.g., low proton density in the lungs producing low MR signal, respiratory and cardiac motion during image acquisition, lack of intrinsic electron density information requiring bulk overrides for the synthetic CT generation, electron return effect being especially pronounced at air-tissue interfaces, and physiological motion during patient setup and treatment. Breath hold imaging, 4D-MRI, gating, and tracking become paramount in order to ensure the tight margins of the PTV and OAR sparing, especially in the cases of the tumors located in the central portion of the thoracic cavity.

Lung tumors have long been a target of SBRT-type treatment that requires increasingly precise delineation of the target and OARs. For instance, the suitability of using the stereotactic magnetic-resonance-guided radiation therapy (SMART) has been investigated by Finazzi et al. [17] on 25 patients with centrally located lung tumors where soft tissue delineation is especially important due to proximity of the heart, esophagus, bronchial tree, and major vessels. MRIdian ViewRay 0.35 T LINAC has been used in these studies. Before each fraction, a breath-hold 3D MR scan was acquired to define the anatomy of the day. The registration would be performed and the physician could then adjust the GTV and the OAR contours as needed. Online plans were reoptimized with the MRIdian planning software using the same beam parameters and optimization objectives. In 92% of cases, the physician chose to proceed with the adapted plans. Treatment delivery occurred during the breath-holds. The optimized plans provided clinically meaningful improvement in the PTV coverage and were able to avoid high doses in the stomach, vertebral bodies, and brachial plexus. PTV dose escalation with the simultaneous OAR sparing was feasible with the provided SMART workflow. A longer study performed by the same group on 54 patients was followed up by 2-year observation period [18]. The use of the SMART workflow did not compromise the tumor control while significantly reducing the toxicity of the treatment, including for patients with previous radiation treatment or resection. No high-grade bronchial toxicity common for the patients with central lung tumor was observed. Much smaller tumor volumes could be used. The results were used to devise a single fraction stereotactic ablative body radiotherapy (SABR) approach for early stage cancer [19]. Ten patients were selected for the study. On the day of treatment, the GTV contours were adjusted by the physicians. On mid-treatment 3D-MR scans, the plans were reoptimized in order to better control dose to the OARs and decrease the hotspot. The patients were observed for 1-year post-SABR, with one patient developing a myocardial infraction. For the remaining nine patients, no grade 3–5 toxicities (according to Common Terminology Criteria for Adverse Effects; CTCAE) and no local recurrences have been observed. Similar results were observed for a single fraction 34 Gy SBRT treatment performed by Chuong et al. [20]. When it comes to Elekta Unity MR-Linac system, Winkel et al. [21] performed a study on 10 patients with ultracentral tumors treated with a hypofractionated schema of 60 Gy in 8–12 fx. All treatments have been well tolerated by patients. A summary of the clinical experience to date has been presented by Crockett et al. [22] (Table 7.1):

The heart provides an even harder target to irradiate as the rapid nature of the human heartbeat makes gating difficult. Nevertheless, several groups have made the attempts to utilize MRI-guided radiation therapy for the treatment of various conditions of the heart. For instance, Pomp et al. [28] report the treatment of the sarcoma

Table 7.1 MRgRT of primary lung tumors and pulmonary metastases, clinical experience to date

Team	Machine	No. of patients	Tumor location	Fractionation schedule	Adaptation	Gating/ tracking	Couch time (min)
Thomas et al. [23]	MRIdian Cobalt-60	5	Peripheral and central	50–54 Gy/3–4 fx	NR	Tracking	>20
Padgett et al. [24]	MRIdian Cobalt-60	3 (one primary lung)	Peripheral	50 Gy/5 fx	To anatomy	NR	NR
De Costa et al. [25]	MRIdian Cobalt-60	14 (11 primary lung)	NR	40–50 Gy/5 fx	NR	Both	NR
Henke et al. [26]	MRIdian Cobalt-60	5 (one primary lung)	Ultra-central	50 Gy/5 fx	To anatomy	Gating	Median = 69
Finazzi et al. [27]	MRIdian Cobalt-60 or MR-Linac	23 (25 tumors, 14 primary lung)	Peripheral	54–60 Gy/3–8 fx	To anatomy	Gating	Median Cobalt-60 = 62; MR-Linac = 48
Finazzi et al. [19]	MRIdian MR-Linac	10 (eight primary lung)	Peripheral	34 Gy/1 fx	To anatomy	Both	Median = 120 min
Finazzi et al. [18]	MRIdian Cobalt-60 or MRI Linac	50 (29 primary lung)	Peripheral and central	54–60 Gy/3–12 fx	To anatomy	Both	Median Cobalt-60 = 60; MR-Linac = 49
Lung metastases							
Henke et al. [26]	MRIdian Cobalt-60	5 (four oligometastases)	Ultra-central	50 Gy/5 fx	To anatomy	Gating	Median = 69
Finazzi et al. [27]	MRIdian Cobalt-60 or MR- Linac	23 (25 tumors, 11 oligometastases)	Peripheral	54–60 Gy/3–8 fx	To anatomy	Gating	Median Cobalt-60 = 62, MR-Linac = 48
Finazzi et al. [19]	MRIdian MR-Linac	10 (two oligometastases)	Peripheral	34 Gy/1 fx	To anatomy	Both	Median = 120
Finazzi et al. [18]	MRIdian Cobalt-60 or MRI Linac	50 (21 oligometastases)	Peripheral and central	54–60 Gy/3–12 fx	To anatomy	Both	Median Cobalt-60 = 60; MR-Linac = 49

Adapted from: Crockett, C. B., Samson, P., Chuter, R., Dubec, M., Faivre-Finn, C., Green, O. L., & Cobben, D. (2021). Initial clinical experience of MR-guided radiotherapy (MRgRT) for nonsmall cell lung cancer (NSCLC). Frontiers in Oncology, 11, 157

of the heart. The patient had already experienced recurrent strokes and a cardiac surgery before the radiation treatment took place to control a recurrent nonresectable tumor. As only the portion of the heart containing tumor was irradiated, the remaining healthy heart, along with lungs, esophagus, and bronchi were treated as OARs. SBRT-type treatment with 60 Gy delivered in 12 fx with online adaptation was performed and well tolerated. Another case study was described by Gach et al. [29]. The patient in question had cardiac fibroma, as well as an implantable cardioverter defibrillator, making treatment planning and delivery an additional challenge. The patient had an MR-compatible Medtronic Evera Surescan ICD, and, according to the cardiologist assessment, was not device-dependent, presenting standard medium-risk. All the MRI conditions were confirmed with a vendor, with all of them being met with the exception of the use of the device in the presence of the 0.35-T magnetic field, as the device was tested in 1.5-T field conditions. The off-label use of the device was assessed by the medical physicist and discussed with the patient, and several adjustments to the device operation mode were made based on vendor's recommendations. The presence of the ICD on the MR images caused null band artifacts that ran through the heart. Nevertheless, the attending physician was able to successfully identify the target and make the GTV adjustments as needed for the gating purposes. The patient reported no pain during the treatment and was not in cardiac distress. The device appeared to be undamaged by the MRI scans or the radiation.

A separate study was presented by Sim et al. [30] where the MR-guided radiation therapy was considered for the treatment of intracardiac and pericardial metastases. Five patients were selected for the study, including two with pre-existent cardiac disease. SBRT-type treatment with 40–50 Gy delivered over the course of 5 fx was prescribed. In this scenario, the representative slice of the lesion was contoured on each day and used for the gating purposes. No plan adaptation was used for the patients. All symptomatic patients experienced some relief postirradiation, and there were no acute adverse effects; however, one of the patients without prior cardiac disease ended up developing atrial defibrillation 6 months after treatment. An adaptation of the treatment plan was considered to be a viable plan as a result of the study based on the observed workflow.

Esophageal tumors in the thoracic cavity also present a unique challenge. Boekhoff et al. [31] discuss the reduction of the dose to the heart, large vessels, trachea, bronchial tree, and lungs with the help of the adaptive MR-guided radiation therapy on a study consisting of 32 patients with the esophageal cancers. This study did not contain any cases of the prior irradiation and surgery. Daily GTV changes were evaluated based on the acquired on-board MR imaging. Considerable day-to-day shape changes of the clinical target volume (CTV) were observed. The target coverage was most often compromised on the distal part of the CTV, near the gastroesophageal junction and into the cardia. The changes could not be accounted for by translation and rotation only, and required on-table adaptive workflow with daily regeneration of the new plans. Winkel et al. [21] and Lee at al [32]. reach similar conclusion. In addition to the day-to-day positional variation of the location of the GTV and CTV, the esophageal cancer GTV tends to shrink significantly as the treatment progresses, with the tumors decreasing up to 28% by the fifth week, thus also necessitating the radiation treatment plan adjustment [33]. When it comes to respiratory gating

management, lower esophageal tumors experience the largest range of motion associated with breathing pattern due to the proximity of the diaphragm.

7.2.4 Abdominal Tumors

Abdominal structures have long been a challenge to a traditional CT-based approach due to the low soft tissue contrast. MR-guided radiation treatment provides a unique opportunity to differentiate between the abdominal structures, allowing for the better OAR sparing and potential dose escalation to the mobile tumors in abdomen. Various treatment sites in the abdominal cavity have been considered for MR-guided radiation therapy, with liver and pancreas being the most attractive targets. Bohoudi et al. [34] suggested the adaptive workflow and evaluated the margins within which the recountouring was required in order to ensure the same or better OAR sparing and target control as with the full contouring, determining that a 3-cm ring around the PTV was sufficient for the clinical purposes for the abdominal targets. In their later publication, Bohoudi et al. [35] also presented the analysis of the criteria of patient selection for the adaptive radiation therapy. Plan adaptation appeared to be relevant mainly in cases where the GTV to adjacent OAR distance was <3 mm. These criteria were evaluated on the example of pancreatic cancer but were later adopted as a strategy for all abdominal cancers. One of the earliest studies has been conducted by Henke et al. [36] in 2017 on the MRIdian ViewRay Linac system. Twenty patients with oligometastatic or unresectable primary abdominal malignancies, including 10 patients with liver tumors, and 10 patients with nonliver tumors, received 50 Gy in 5 fx, with each fraction following the adapt-to-shape workflow that allowed for the complete plan adaptation based on the daily anatomy variation. The patients were observed for 6 months, with zero grade 3 (acc. To CTCAE) acute treatment-related toxicities observed. Several years later, a similar study was repeated for the Elekta Unity MR-LINAC machine, this time with free-breathing abdominal SBRT [37]. Both adapt-to-shape and adapt-to-position workflows were considered. Due to software limitation, an offline Monaco system was used for adaptive plan generation in Adapt-To-Shape (ATS) workflow. Likewise, the study confirmed the feasibility of the MR-guided radiation therapy adaptive workflow for the abdominal cases. Palliative abdominal cases have also been at attractive target for the adaptive radiation therapy. Green et al. [38] presented a case of a nonsmall metastatic lung cancer patient who has experienced a gastrointestinal hemorrhage requiring transfusion. Patient was ineligible for surgery, and an urgent course of radiation treatment of 25 Gy in 5 fx was prescribed. Due to urgency, simulation and the first fraction of treatment occurred on the same day, with 30-min, free breathing, volumetric MRI being acquired and used as the primary planning image. Daily image acquisition and plan adaption based on the anatomy variation were conducted. After completion of the treatment, the patient reported resolution of melena, his hemoglobin improved without subsequent transfusion required, and no toxicity following 3 month was reported. Another case presented in the same report concerns an omental metastatic lesion with high degree of movement in extremely short periods of time. The CT scans taken in the morning and in the afternoon showed a

different location of the lesion, and a decision has been made to perform an MRI simulation with a moving field of view from upper mid-abdomen to pelvis, and to adapt plan "on the fly". The location of the nodule was finally identified, allowing to proceed with treatment. The lesion exhibited a significant change in the position throughout all five fractions, moving at least 2 cm a day (3 cm average) and had a maximum lateral movement of 5 cm. Thus, it would be nearly impossible to treat the patient without daily adaptation. One year after treatment completion, patient exhibited no further growth of the omental lesion and no acute or late abdominopelvic toxicities. Both of these cases presented the motion of the tumors far beyond the boundary of the commonly used PTVs, especially for SBRT-type treatment. Similar case was reported for a stomach cancer by Chun et al. [39]. Stomach is one of the most deforming organs due to respiratory motion and differences in food intake on day-to-day basis. A patient with multiple comorbidities, including end-stage renal disease and liver cirrhosis, and a history of prior distal gastrectomy thus presented a challenging case. Due to the high anatomical variability, daily adjustments of the target volume and OARs were required. The adaptive treatment process took less than 30 min overall. Patient only experienced CTCAE grade 1 nausea throughout the treatment sessions, and the tumor was nearly resolved on post real-time endoscopic evaluation.

An example of the typical isodose coverage for the abdominal tumor treatment is presented on the following figure (Fig. 7.2).

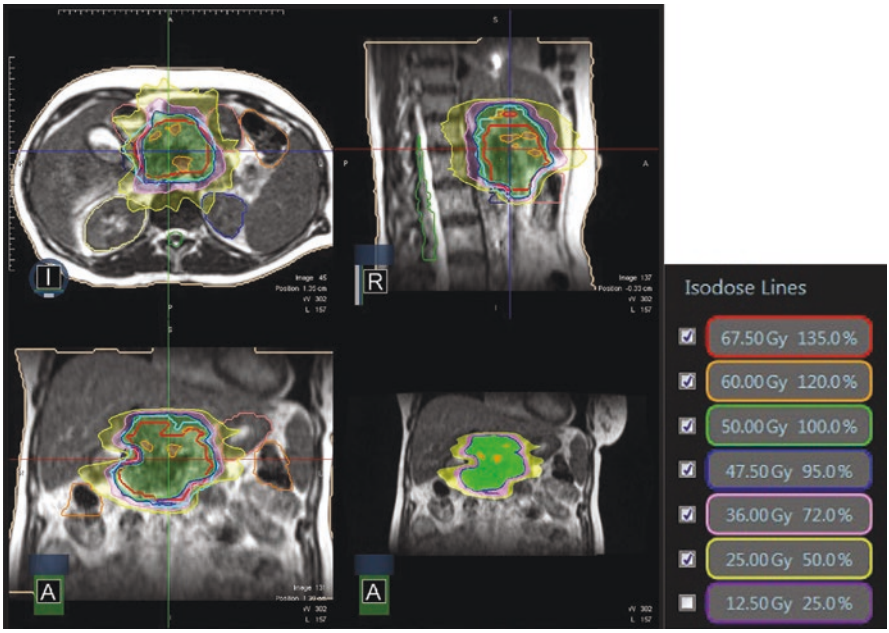

Fig. 7.2 Isodose lines of a radiation treatment plan for a pancreatic adenocarcinoma patient delivered on an MR-LINAC. The plan is depicted in transverse, sagittal, and frontal view, and isodose lines presented in various colors

As can be seen on Fig. 7.2, typical OARs of particular concern usually include duodenum, bowel, stomach, and kidneys. Spinal cord is usually less affected, but nevertheless care should be taken not to let the static beams go directly through the cord during the planning process.

When it comes to the particular organs, liver perhaps takes the lead of being the most common target for the adaptive treatment. For patient with compromised liver function, few local treatment options are available, with chemoembolization and radioembolization being highly dependent on the liver function and lung shunting percentage, with external radiation treatment being left as an only option. Numerous studies confirm the feasibility of using MR-guided radiation treatment for liver lesions, including hepatocellular carcinoma, cholangiosarcomas, metastasis of the neuroendocrine tumors, colorectal carcinomas, and gastrointestinal stroma tumors [40–44]. Boldrini et al. [45] provide a summary of the recent clinical studies on the role of MR-guided radiation therapy in various institutions (Table 7.2).

For the illustrative purposes, an example of the treatment plan for the tumor located in the liver is provided in Fig. 7.3.

Table 7.2 Recent clinical studies on the role of MRgRT in hepatic malignancies

Reference	Year	Dose	No. of patients	Response
Henke et al. [36]	2018	50 Gy/5 fx	Ten nonliver abdomen lesions, six MLL, four HCC	3 months LPFS 95%, 6 months LPFS 89.1%, 1 year OS 75%
Feldman et al. [42]	2019	45–50 Gy/5 fx	26 HCC, two cholangiocarcinoma	1 year LC 96.5%, 1 year OS 92.8%
Rosenberg et al. [43]	2019	Median dose 50 (30–60) Gy/3–5 fx	Six MLL, six HCC, 20 MLL	1 year OS 69%, 2 year OS 60%
Hal et al. [44]	2020	Median dose 45 (25–60 Gy)/3–5 fx	Three pancreatic cancer, two HCC, one pancreatic metastasis, four MLL	7.2 months LC 100%
Luterstein et al. [46]	2020	40 Gy/5 fx	17 cholangiocarcinoma	1 year OS 76%, 2 year OS 46.1%, 1 year LC 85.6%, 2 year LC 73.3%
Boldrini et al. [40]	2021	50–55 Gy/5 fx	Ten HCC	6.5 months LC 90%
ClinicalTrials.gov. NCT0424342 [47]	2019-recruiting	50–60 Gy/5–6 fx	46 primary or secondary liver tumors	2 year LC lack of progression according to RECIST criteria

Adapted from: Boldrini, L., Corradini, S., Gani, C., Henke, L., Hosni, A., Romano, A., & Dawson, L. (2021). MR-guided radiotherapy for liver malignancies. Frontiers in Oncology, 11, 1053

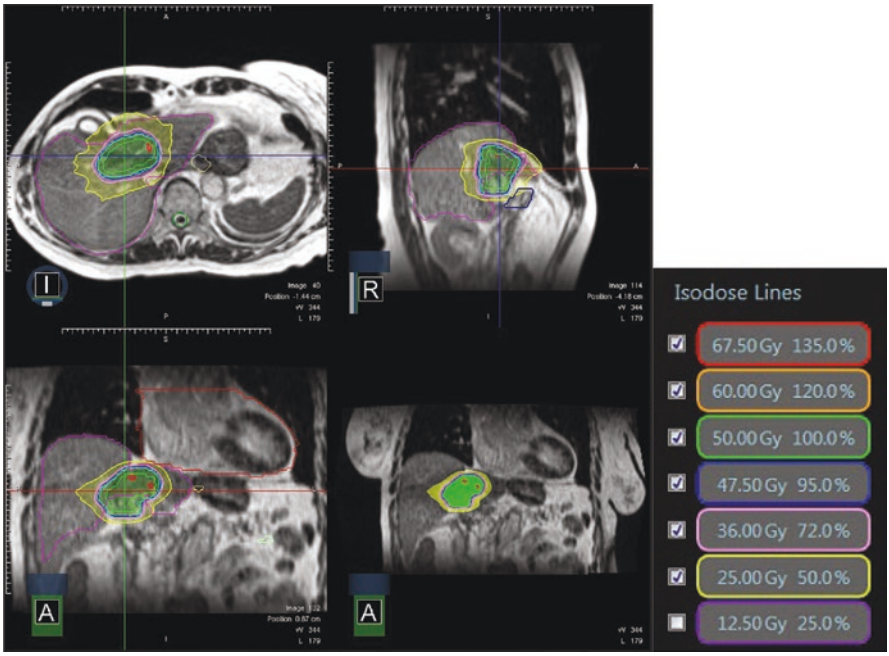

Fig. 7.3 Isodose lines of a radiation treatment plan for a liver tumor patient delivered on an MR-LINAC. The plan is depicted in transverse, sagittal, and frontal view, and isodose lines presented in various colors

An atlas of OAR contouring in the upper abdomen has been published by Lukovic et al. [48] to provide the reference for adaptive radiation therapy for liver malignancies. The use of contrast agents, especially gadoxetic acid, is especially advantageous as it highlights the liver, improving the contrast between healthy and tumorous tissue [49]. Superparamagnetic iron oxide (SPIO) also provides superior liver tumor contrast, particularly in 0.35 T field, as described by Hama et al. [50]. MR compatible fiducial markers, particularly platinum-based, might also be advantageous. In addition, various sequences can be used depending on the type of malignancy, as noted by Namasivayam et al. [51]. Will et al. [52] provide a thorough review of the current state of various approaches to the treatment of liver malignancies, highlighting the importance of the MRI-guided workflow with online adaptation in dose escalation and OAR sparing when facing large anatomical changes on the day-to-day basis. The reduction in toxicity due to online adaptation has been remarkable. In addition, authors suggest that the future venues of research might enable the use of learning neural networks to predict the probability of toxicity, extract the radiomic features, and thus reduce the need for biopsies, and, when combined with genetic factors and tumor microenvironment information, allow to customize radiation dose to different portions of the tumor and allow for prescription variation on the day-to-day basis.

Pancreas is another target of the adaptive radiation treatment that has been attracting a lot of attention in the recent years. Notoriously difficult to detect and often unresectable, it has long been characterized by high lethality and difficulties in finding a treatment approach. Decreased toxicity and improved accuracy offered by the adaptive MR-guided workflow provide a treatment solution to previously untreatable cases. Hassandazeh et al. [53] presented a study on 44 patients with inoperable pancreatic cancer treated over the course of five years (2014–2019) with 50 Gy in 5 fx. Majority of the patients had the tumor either abutting or invading the OARs. Late toxicity was limited to two grade 3 and three grade 2 (acc. to CTCAE) toxicities. Median overall survival was 15.7 months, with one-year local control reaching 84.3%. The minimization of toxicity allowed for significant dose escalation and improved tumor control. Similar results were reported by Rudra et al. [54], with higher overall survival being reported for patients with escalated dose regimen.

Adrenal and renal metastases are also a frequent target of MR-guided adaptive radiotherapy. In a study by Palacios et al. [55], 17 patients who were deemed poor candidates for a traditional surgical approach were evaluated, with plan adaptation required due to significant OAR displacement. Primary renal cell cancer treatment with the use of MR-guided adaptive radiation therapy has been reported by Rudra et al. [56], Tetar et al. [57], Kutuk et al. [58], with varying doses, all demonstrating good tumor control in addition to decreased toxicity to the OARs. This is consistent with the treatment results observed for other abdominal sites.

7.2.5 Pelvic Tumors

The anatomy of the pelvis, while undergoing less changes on the day-to-day basis than the abdominal cavity, and not susceptible to the breathing-induced movement, can nevertheless present a challenge for the daily positioning. Soft tissue contrast provided by the MR-based imaging allows for better target localization. Several sites have been considered for the feasibility of using MR-guided radiation therapy with adapted workflow, with prostate being the most promising candidate. Improved local control and decreased toxicity allow for hypofractionated treatment with a significant dose escalation. Bruynzeel et al. [59] presented one of the first comprehensive studies conducted on 101 patients with T1-3bN0M0 prostate cancer, with no fiducial markers implanted, requiring daily adaptation of the OARs and the PTV localization. Clinically comparable local control and significantly reduced GI toxicity were observed. Urethral sparing was particularly noticeable compared to the normal workflow. A later study on the same patient study was performed to investigate the possible late-term toxicity [60]. All of the urinary and bowel syndromes resolved within 12 months. The same group later investigated the drift of the extent of the intrafractional prostate drift, which was exhibited in 20% of the cases [61]. Similar results were reported by Mazolla et al. [62] for oligometastatic cancer. Several groups have attempted to implement MR-guided SBRT regimen, with the results summarized in the following table [63] (Table 7.3).

Table 7.3 Literature experience of MRgRT for prostate cancer

Author	No. of patients	MR-Linac device	Fractionation schedule	Endpoint of the study	Results
Alongi et al. [64]	20	Elekta Unity	35 Gy/5 fx	Dosimetric analysis and preliminary PROMs report	Hydrogel improves rectal sparing with minimal impact on QoL
Bruynzeel et al. [59]	101	ViewRay MRIdian	36.25 Gy/5 fx	Early toxicity analysis	G > 2 GU = 23.8%, ≥2 GI = 5%
Cuccia et al. [65]	20	Elekta Unity	35 Gy/5 fx	Assessment of the impact of rectal spacer on prostate motion	Significant impact on rotational antero-posterior shifts with consequently reduced prostate motion
Tetar et al. [60]	101	ViewRay MRIdian	36.25 Gy/5 fx	PROMs analysis	After one year, only 2.25 of cases reported relevant impact to daily activities due to GU toxicity
Nicosia et al. [66]	10	Elekta Unity	35 Gy/5 fx	Dosimetric comparison between MR-guided SBRT and conventional LINAC SBRT	MR-guided SBRT resulted in lower constraint violation rates
Sahin et al. [67]	24	ViewRay MRIdian	36.25 Gy/5 fx	Preliminary report of feasibility	Substantial feasibility of MR-adaptive SBRT with acceptable time schedules
Ugurluer at al [68]	50	ViewRay MRIdian	36.25 Gy/5 fx	Early toxicity analysis	Acute G2 GU = 28%, late G2 GU = 6%, late GI GU = 2%

Adapted from: Cuccia, F., Corradini, S., Mazzola, R., Spiazzi, L., Rigo, M., Bonù, M. L., ... & Alongi, F. (2021). MR-guided hypofractionated radiotherapy: current emerging data and promising perspectives for localized prostate cancer. Cancers, 13(8), 1791

The possibility of further margin reduction and single-shot treatment is currently being considered in prostate cancer. Possibility of the sexual function preservation might also become possible as the MR-guided radiation therapy provides a better sparing of the healthy tissue. This can also be an exciting prospect for the re-irradiation cases.

Cervical cancer can also benefit from MR-guided radiation therapy. Boldrini et al. [69] presented the first study conducted on eight patients that was compared to the results of the treatment on a conventional linear accelerator. A significant

reduction in both gastrointestinal and genitourinary toxicities was observed for the patients undergoing MR-guided radiation treatment, with no difference in pathological response observed between the two groups. This is consistent with the results observed for prostate cancer treatment.

Ovarian cancer can also benefit from MR-guided radiation therapy. A study presented by Henke et al. [70] covers ten patients, initially prescribed 35 Gy in 5 fx, with dose escalation permitted subject to strict OAR dose constraints. Only a single grade 3 toxicity was observed. Local control at 3 months reached 94%.

Rectum is an organ that experiences significant day-to-day deformation, and rectal wall can also be difficult to trace exactly on the cone-beam computed tomography (CBCT). MRI provides better soft tissue contrast and enables exact GTV localization. While the speculation of the use of MR-guided workflow has been present in the literature, as of this moment, only one study has been presented. Chiloiro et al. [71] conducted a study on 22 patients with colorectal cancer, with 86% exhibiting nodal involvement. As a result of the therapy, five patients reached grade 3 gastrointestinal toxicity. No grade 3 hematologic or genitourinary toxicity was observed. Improved local tumor control was observed.

Bladder is another target that is susceptible to significant anatomical changes. In addition, MR imaging allows the visualization of the bladder muscle layer otherwise invisible on the CT. Hijab et al. [72] discuss the potential MR-guided adaptive workflow for bladder cancers, though as of this moment, no thorough study has been conducted on a patient set.

Overall, the MR-guided radiation therapy presents a promising venue for the exploration of new treatment regimens. Additional studies with a larger number of patients are being conducted on various sites across the world, and with MR-equipped linear accelerators becoming more and more widely spread, it can soon become a standard of care. New developments are highly anticipated in the upcoming years.

References

1. Green OL, Henke LE, Hugo GD. Practical clinical workflows for online and offline adaptive radiation therapy. Semin Radiat Oncol. 2019;29(3). WB Saunders
2. Hall WA, Paulson ES, van der Heide UA, Fuller CD, Raaymakers BW, Lagendijk JJ, et al. The transformation of radiation oncology using real-time magnetic resonance guidance: a review. Eur J Cancer. 2019;122:42–52.
3. Otazo R, Lambin P, Pignol JP, Ladd ME, Schlemmer HP, Baumann M, Hricak H. MRI-guided radiation therapy: an emerging paradigm in adaptive radiation oncology. Radiology. 2021;298(2):248–60.
4. Glide-Hurst CK, Lee P, Yock AD, Olsen JR, Cao M, Siddiqui F, et al. Adaptive radiation therapy (art) strategies and technical considerations: a state of the art review from nrg oncology. Int J Radiat Oncol Biol Phys. 2021;109(4):1054–75.
5. Mehta S, Gajjar SR, Padgett KR, Asher D, Stoyanova R, Ford JC, Mellon EA. Daily tracking of glioblastoma resection cavity, cerebral edema, and tumor volume with MRI-guided radiation therapy. Cureus. 2018;10(3):e2346.
6. Tsien C, Gomez-Hassan D, Ten Haken RK, Tatro D, Junck L, Chenevert TL, Lawrence T. Evaluating changes in tumor volume using magnetic resonance imaging during the course

of radiotherapy treatment of high-grade gliomas: implications for conformal dose-escalation studies. Int J Radiat Oncol Biol Phys. 2005;62(2):328–32.
7. Shukla D, Huilgol NG, Trivedi N, Mekala C. T2-weighted MRI in assessment of volume changes during radiotherapy of high-grade gliomas. J Cancer Res Ther. 2005;1(4):235.
8. Yang Z, Zhang Z, Wang X, Hu Y, Lyu Z, Huo L, et al. Intensity-modulated radiotherapy for gliomas: dosimetric effects of changes in gross tumor volume on organs at risk and healthy brain tissue. Onco Targets Ther. 2016;9:3545.
9. Maziero D, Straza MW, Ford JC, Bovi JA, Diwanji T, Stoyanova R, et al. MR-guided radiotherapy for brain and spine tumors. Front Oncol. 2021;11:600.
10. Spieler B, Samuels SE, Llorente R, Yechieli R, Ford JC, Mellon EA. Advantages of radiation therapy simulation with 0.35 tesla magnetic resonance imaging for stereotactic ablation of spinal metastases. Pract Radiat Oncol. 2020;10(5):339–44.
11. Boeke S, Mönnich D, Van Timmeren JE, Balermpas P. MR-guided radiotherapy for head and neck cancer: current developments, perspectives, and challenges. Front Oncol. 2021;11:429.
12. Chen AM, Hsu S, Lamb J, Yang Y, Agazaryan N, Steinberg ML, et al. MRI-guided radiotherapy for head and neck cancer: initial clinical experience. Clin Transl Oncol. 2018;20(2):160–8.
13. Chamberlain M, Krayenbuehl J, van Timmeren JE, Wilke L, Andratschke N, Schüler HG, et al. Head and neck radiotherapy on the MR linac: a multicenter planning challenge amongst MRIdian platform users. Strahlenther Onkol. 2021:1–11.
14. Gurney-Champion OJ, McQuaid D, Dunlop A, Wong KH, Welsh LC, Riddell AM, et al. MRI-based assessment of 3D Intrafractional motion of head and neck cancer for radiation therapy. Int J Radiat Oncol Biol Phys. 2018;100(2):306–16.
15. Bruijnen T, Stemkens B, Terhaard CH, Lagendijk JJ, Raaijmakers CP, Tijssen RH. Intrafraction motion quantification and planning target volume margin determination of head-and-neck tumors using cine magnetic resonance imaging. Radiother Oncol. 2019;130:82–8.
16. McDonald BA, Vedam S, Yang J, Wang J, Castillo P, Lee B, et al. Initial feasibility and clinical implementation of daily MR-guided adaptive head and neck cancer radiation therapy on a 1.5 T MR-Linac system: prospective R-IDEAL 2a/2b systematic clinical evaluation of technical innovation. Int J Radiat Oncol Biol Phys. 2021;109(5):1606–18.
17. Finazzi T, Palacios MA, Spoelstra FO, Haasbeek CJ, Bruynzeel AM, Slotman BJ, et al. Role of on-table plan adaptation in MR-guided ablative radiation therapy for central lung tumors. Int J Radiat Oncol Biol Phys. 2019;104(4):933–41.
18. Finazzi T, Haasbeek CJ, Spoelstra FO, Palacios MA, Admiraal MA, Bruynzeel AM, et al. Clinical outcomes of stereotactic MR-guided adaptive radiation therapy for high-risk lung tumors. Int J Radiat Oncol Biol Phys. 2020;107(2):270–8.
19. Finazzi T, de Koste JRVS, Palacios MA, Spoelstra FO, Slotman BJ, Haasbeek CJ, Senan S. Delivery of magnetic resonance-guided single-fraction stereotactic lung radiotherapy. Phys Imaging Radiat Oncol. 2020;14:17–23.
20. Chuong MD, Kotecha R, Mehta MP, Adamson S, Romaguera T, Hall MD, et al. Case report of visual biofeedback-driven, magnetic resonance-guided single-fraction SABR in breath hold for early stage non–small-cell lung cancer. Med Dosim. 2021;46(3):247–52.
21. Winkel D, Bol GH, Kroon PS, van Asselen B, Hackett SS, Werensteijn-Honingh AM, et al. Adaptive radiotherapy: the Elekta Unity MR-linac concept. Clin Translat Radiat Oncol. 2019;18:54–9.
22. Crockett CB, Samson P, Chuter R, Dubec M, Faivre-Finn C, Green OL, et al. Initial clinical experience of MR-guided radiotherapy (MRgRT) for non-small cell lung cancer (NSCLC). Front Oncol. 2021;11:157.
23. Thomas DH, Santhanam A, Kishan AU, Cao M, Lamb J, Min Y, et al. Initial clinical observations of intra-and interfractional motion variation in MR-guided lung SBRT. Br J Radiol. 2018;91(xxxx):20170522.
24. Padgett KR, Simpson GN, Llorente R, Samuels MA, Dogan N. Feasibility of adaptive MR-guided stereotactic body radiotherapy (SBRT) of lung tumors. Cureus. 2018;10(4):e2423.

25. De Costa AMA, Mittauer KE, Hill PM, Bassetti MF, Bayouth J, Baschnagel AM. Outcomes of real-time MRI-guided lung stereotactic body radiation therapy. Int J Radiat Oncol Biol Phys. 2018;102(3):e679–80.
26. Henke LE, Olsen JR, Contreras JA, Curcuru A, DeWees TA, Green OL, et al. Stereotactic MR-guided online adaptive radiation therapy (SMART) for ultracentral thorax malignancies: results of a phase 1 trial. Adv Radiat Oncol. 2019;4(1):201–9.
27. Finazzi T, Palacios MA, Haasbeek CJ, Admiraal MA, Spoelstra FO, Bruynzeel AM, et al. Stereotactic MR-guided adaptive radiation therapy for peripheral lung tumors. Radiother Oncol. 2020;144:46–52.
28. Pomp J, van Asselen B, Tersteeg RH, Vink A, Hassink RJ, van der Kaaij NP, et al. Sarcoma of the heart treated with stereotactic MR-guided online adaptive radiation therapy. Case Rep Oncol. 2021;14(1):453–8.
29. Michael Gach H, Curcuru AN, Wittland EJ, Maraghechi B, Cai B, Mutic S, Green OL. MRI quality control for low-field MR-IGRT systems: lessons learned. J Appl Clin Med Phys. 2019;20(10):53–66.
30. Sim AJ, Palm RF, DeLozier KB, Feygelman V, Latifi K, Redler G, et al. MR-guided stereotactic body radiation therapy for intracardiac and pericardial metastases. Clin Translat Radiat Oncol. 2020;25:102–6.
31. Boekhoff MR, Defize IL, Borggreve AS, Takahashi N, van Lier ALHMW, Ruurda JP, et al. 3-Dimensional target coverage assessment for MRI-guided esophageal cancer radiotherapy. Radiother Oncol. 2020;147:1–7.
32. Lee SL, Bassetti M, Meijer GJ, Mook S. Review of MR-guided radiotherapy for esophageal cancer. Front Oncol. 2021;11:468.
33. Defize IL, Boekhoff MR, Borggreve AS, van Lier AL, Takahashi N, Haj Mohammad N, et al. Tumor volume regression during neoadjuvant chemoradiotherapy for esophageal cancer: a prospective study with weekly MRI. Acta Oncol. 2020;59(7):753–9.
34. Bohoudi O, Bruynzeel AME, Senan S, Cuijpers JP, Slotman BJ, Lagerwaard FJ, Palacios MA. Fast and robust online adaptive planning in stereotactic MR-guided adaptive radiation therapy (SMART) for pancreatic cancer. Radiother Oncol. 2017;125(3):439–44.
35. Bohoudi O, Bruynzeel AM, Meijerink MR, Senan S, Slotman BJ, Palacios MA, Lagerwaard FJ. Identification of patients with locally advanced pancreatic cancer benefitting from plan adaptation in MR-guided radiation therapy. Radiother Oncol. 2019;132:16–22.
36. Henke L, Kashani R, Robinson C, Curcuru A, DeWees T, Bradley J, et al. Phase I trial of stereotactic MR-guided online adaptive radiation therapy (SMART) for the treatment of oligometastatic or unresectable primary malignancies of the abdomen. Radiother Oncol. 2018;126(3):519–26.
37. Paulson ES, Ahunbay E, Chen X, Mickevicius NJ, Chen GP, Schultz C, et al. 4D-MRI driven MR-guided online adaptive radiotherapy for abdominal stereotactic body radiation therapy on a high field MR-Linac: implementation and initial clinical experience. Clin Translat Radiat Oncol. 2020;23:72–9.
38. Green OL, Henke LE, Price A, Marko A, Wittland EJ, Rudra S, et al. The role of MRI-guided radiation therapy for palliation of Mobile abdominal cancers: a report of two cases. Adv Radiat Oncol. 2021;6(4):100662.
39. Chun SJ, Jeon SH, Chie EK. A case report of salvage radiotherapy for a patient with recurrent gastric cancer and multiple comorbidities using real-time MRI-guided adaptive treatment system. Cureus. 2018;10(4):e2471.
40. Boldrini L, Romano A, Mariani S, Cusumano D, Catucci F, Placidi L, et al. MRI-guided stereotactic radiation therapy for hepatocellular carcinoma: a feasible and safe innovative treatment approach. J Cancer Res Clin Oncol. 2021;147(7):2057–68.
41. Rogowski P, von Bestenbostel R, Walter F, Straub K, Nierer L, Kurz C, et al. Feasibility and early clinical experience of online adaptive MR-guided radiotherapy of liver tumors. Cancers. 2021;13(7):1523.

42. Feldman AM, Modh A, Glide-Hurst C, Chetty IJ, Movsas B. Real-time magnetic resonance-guided liver stereotactic body radiation therapy: an institutional report using a magnetic resonance-linac system. Cureus. 2019;11(9):e5774.
43. Rosenberg SA, Henke LE, Shaverdian N, Mittauer K, Wojcieszynski AP, Hullett CR, et al. A multi-institutional experience of MR-guided liver stereotactic body radiation therapy. Adv Radiat Oncol. 2019;4(1):142–9.
44. Hal WA, Straza MW, Chen X, Mickevicius N, Erickson B, Schultz C, et al. Initial clinical experience of Stereotactic Body Radiation Therapy (SBRT) for liver metastases, primary liver malignancy, and pancreatic cancer with 4D-MRI-based online adaptation and real-time MRI monitoring using a 1.5 Tesla MR-Linac. PLoS One. 2020;15(8):e0236570.
45. Boldrini L, Corradini S, Gani C, Henke L, Hosni A, Romano A, Dawson L. MR-guided radiotherapy for liver malignancies. Front Oncol. 2021;11:1053.
46. Luterstein E, Cao M, Lamb JM, Raldow A, Low D, Steinberg ML, Lee P. Clinical outcomes using magnetic resonance–guided stereotactic body radiation therapy in patients with locally advanced cholangiocarcinoma. Adv Radiat Oncol. 2020;5(2):189–95.
47. Centre Georges Francois Leclerc. Phase II of Adaptative Magnetic Resonance-Guided Stereotactic Body Radiotherapy (SBRT) for Treatment of Primary or Secondary Progressive Liver Tumors. clinicaltrials.gov (2020). https://clinicaltrials.gov/ct2/show/NCT04242342. Accessed 20 Dec 2021.
48. Lukovic J, Henke L, Gani C, Kim TK, Stanescu T, Hosni A, et al. MRI-based upper abdominal organs-at-risk atlas for radiation oncology. Int J Radiat Oncol Biol Phys. 2020;106(4):743–53.
49. Goodwin MD, Dobson JE, Sirlin CB, Lim BG, Stella DL. Diagnostic challenges and pitfalls in MR imaging with hepatocyte-specific contrast agents. Radiographics. 2011;31(6):1547–68.
50. Hama Y, Tate E. Superparamagnetic iron oxide-enhanced MRI-guided stereotactic ablative radiation therapy for liver metastasis. Rep Pract Oncol Radiother. 2021;26(3):470–4.
51. Namasivayam S, Martin DR, Saini S. Imaging of liver metastases: MRI. Cancer Imaging. 2007;7(1):2.
52. Witt JS, Rosenberg SA, Bassetti MF. MRI-guided adaptive radiotherapy for liver tumours: visualising the future. Lancet Oncol. 2020;21(2):e74–82.
53. Hassanzadeh C, Rudra S, Bommireddy A, Hawkins WG, Wang-Gillam A, Fields RC, et al. Ablative five-fraction stereotactic body radiation therapy for inoperable pancreatic cancer using online MR-guided adaptation. Adv Radiat Oncol. 2021;6(1):100506.
54. Rudra S, Jiang N, Rosenberg SA, Olsen JR, Roach MC, Wan L, et al. Using adaptive magnetic resonance image-guided radiation therapy for treatment of inoperable pancreatic cancer. Cancer Med. 2019;8(5):2123–32.
55. Palacios MA, Bohoudi O, Bruynzeel AM, de Koste JRVS, Cobussen P, Slotman BJ, et al. Role of daily plan adaptation in MR-guided stereotactic ablative radiation therapy for adrenal metastases. Int J Radiat Oncol Biol Phys. 2018;102(2):426–33.
56. Rudra S, Fischer-Valuck B, Pachynski R, Daly M, Green O. Magnetic resonance image guided stereotactic body radiation therapy to the primary renal mass in metastatic renal cell carcinoma. Adv Radiat Oncol. 2019;4(4):566.
57. Tetar SU, Bohoudi O, Senan S, Palacios MA, Oei SS, Wel AM, et al. The role of daily adaptive stereotactic MR-guided radiotherapy for renal cell cancer. Cancers. 2020;12(10):2763.
58. Kutuk T, McCulloch J, Mittauer KE, Romaguera T, Alvarez D, Gutierrez AN, et al. Daily online adaptive magnetic resonance image (MRI)-guided stereotactic body radiation therapy for primary renal cell cancer. Med Dosim. 2021;46(3):289–94.
59. Bruynzeel AM, Tetar SU, Oei SS, Senan S, Haasbeek CJ, Spoelstra FO, et al. A prospective single-arm phase 2 study of stereotactic magnetic resonance guided adaptive radiation therapy for prostate cancer: early toxicity results. Int J Radiat Oncol Biol Phys. 2019;105(5):1086–94.
60. Tetar SU, Bruynzeel AM, Oei SS, Senan S, Fraikin T, Slotman BJ, et al. Magnetic resonance-guided stereotactic radiotherapy for localized prostate cancer: final results on patient-reported outcomes of a prospective phase 2 study. Eur Urol Oncol. 2021;4(4):628–34.

61. Tetar SU, Bruynzeel AM, Lagerwaard FJ, Slotman BJ, Bohoudi O, Palacios MA. Clinical implementation of magnetic resonance imaging guided adaptive radiotherapy for localized prostate cancer. Phys Imaging Radiat Oncol. 2019;9:69–76.
62. Mazzola R, Cuccia F, Figlia V, Rigo M, Nicosia L, Giaj-Levra N, et al. Stereotactic body radiotherapy for oligometastatic castration sensitive prostate cancer using 1.5 T MRI-Linac: preliminary data on feasibility and acute patient-reported outcomes. La radiologia medica. 2021;126(7):1–9.
63. Cuccia F, Corradini S, Mazzola R, Spiazzi L, Rigo M, Bonù ML, et al. MR-guided Hypofractionated radiotherapy: current emerging data and promising perspectives for localized prostate cancer. Cancers. 2021;13(8):1791.
64. Alongi F, Rigo M, Figlia V, Cuccia F, Giaj-Levra N, Nicosia L, et al. 1.5 T MR-guided and daily adapted SBRT for prostate cancer: feasibility, preliminary clinical tolerability, quality of life and patient-reported outcomes during treatment. Radiat Oncol. 2020;15(1):1–9.
65. Cuccia F, Mazzola R, Nicosia L, Figlia V, Giaj-Levra N, Ricchetti F, et al. Impact of hydrogel peri-rectal spacer insertion on prostate gland intra-fraction motion during 1.5 T MR-guided stereotactic body radiotherapy. Radiat Oncol. 2020;15(1):1–9.
66. Nicosia L, Sicignano G, Rigo M, Figlia V, Cuccia F, De Simone A, et al. Daily dosimetric variation between image-guided volumetric modulated arc radiotherapy and MR-guided daily adaptive radiotherapy for prostate cancer stereotactic body radiotherapy. Acta Oncol. 2021;60(2):215–21.
67. Sahin B, Mustafayev TZ, Gungor G, Aydin G, Yapici B, Atalar B, Ozyar E. First 500 fractions delivered with a magnetic resonance-guided radiotherapy system: initial experience. Cureus. 2019;11(12):e6457.
68. Ugurluer G, Atalar B, Zoto Mustafayev T, Gungor G, Aydin G, Sengoz M, et al. Magnetic resonance image-guided adaptive stereotactic body radiotherapy for prostate cancer: preliminary results of outcome and toxicity. Br J Radiol. 2021;94(1117):20200696.
69. Boldrini L, Piras A, Chiloiro G, Autorino R, Cellini F, Cusumano D, et al. Low Tesla magnetic resonance-guided radiotherapy for locally advanced cervical cancer: first clinical experience. Tumori J. 2020;106(6):497–505.
70. Henke LE, Stanley JA, Robinson C, Srivastava A, Contreras JA, Curcuru A, et al. Phase I trial of stereotactic MRI-guided online adaptive radiation therapy (SMART) for the treatment of oligometastatic ovarian cancer. Int J Radiat Oncol Biol Phys. 2021;112(2):379–89.
71. Chiloiro G, Boldrini L, Meldolesi E, Re A, Cellini F, Cusumano D, et al. MR-guided radiotherapy in rectal cancer: first clinical experience of an innovative technology. Clin Translat Radiat Oncol. 2019;18:80–6.
72. Hijab A, Tocco B, Hanson I, Meijer H, Nyborg CJ, Bertelsen AS, et al. MR-guided adaptive radiotherapy for bladder cancer. Front Oncol. 2021;11:637591.